

A Simplified Method for Prediction of Ultimate Bearing Capacity of Eccentrically Loaded Foundation on Geogrid Reinforced Sand Bed

Ehsan Badakhshan¹ · Ali Noorzad¹

Received: 8 November 2016 / Accepted: 27 April 2017 / Published online: 10 May 2017
© Springer International Publishing Switzerland 2017

Abstract This study aimed to develop reduction factors for eccentric ultimate bearing capacity of circular and square footings resting on geogrid-reinforced sand. The process has been simplified with presenting non-dimensional charts for the various load eccentricities, the number of reinforcement layers and footing shape, which can be used by practicing engineers directly. To establish and evaluate this approach a series experimental tests for circular and square shallow footings was considered. Regarding square footing, different ratios of load eccentricity were considered; one-way and two-way. The proposed approach for eccentric loading in unreinforced and reinforced condition has been validated with Meyerhof's Effective Width Concept, laboratory model tests and numerical reported data in the literature review. Also, this solution is verified using the results of field tests on actual full scale reinforced soil foundations to study scale effects. New method provides reasonable agreement of the ultimate bearing capacity. Also, the results of laboratory tests conducted by the authors show that the ultimate bearing capacity of circular footing decreases less with increment of load eccentricity in comparison with square footing in reinforced condition. Improvement Index investigated that contribution of reinforcement layers in enhancing the ultimate bearing capacity increases with the load eccentricity. This behaviour followed with the proposed model. Also, finite element

method (FEM) in a three-dimensional space is performed for verifying the laboratory tests and studying the stress-strain behaviour of reinforcement layers.

Keywords Shallow foundations · Reinforced sand · Eccentric loading · Bearing capacity · Reduction factor

Introduction

Most of foundations especially with industrial applications are subjected to horizontal seismic and wind forces that causes eccentric loading. Regarding the cases where loading is applied with eccentricity, a few studies have been developed experimentally to identify the critical values of reinforcement layers for reinforcing of the soil under the strip and rectangular foundations. Sawwaf [1] conducted a series model tests on eccentrically loaded strip footing resting on geogrid reinforced sand and proposed that the effect of reinforced soil on the bearing capacity ratio is greater at lower values of eccentricity and in greater relative densities. They found out that maximum improvement occurred at a depth ratio of $u/B=0.33$ and $h/B=0.5$ where u is the depth of first layer, h is vertical spacing between layers and B is the width of footing. In the same vein, Patra et al. [2] proposed an empirical relationship from model loading tests on an eccentrically loaded strip foundation in geogrid reinforced sand bed. Also, Sadoglo et al. [3] reported that reinforcement increased ultimate loads in comparison with the unreinforced cases and this contribution can become much larger with increasing of load eccentricity. Many researchers [4–12] reported that for strip footings the optimum values of u/B for the first geogrid layer varies from 0.35 to 0.45, depending on the value of

✉ Ehsan Badakhshan
E_Badakhshan@sbu.ac.ir
<http://www.sbu.ac.ir>

Ali Noorzad
A_Noorzad@sbu.ac.ir

¹ Faculty of Civil, Water & Environmental Engineering, Shahid Beheshti University, Tehran, Iran

load eccentricity. In addition, several researchers such as Michalowski and You [13], Mahiyar and Patel [14], Patra et al. [2] and Saran et al. [15, 16] investigated the behavior of the square and rectangular foundations under eccentric loading. Sawaf and Nazir [17] studied the behavior of eccentrically loaded small scale ring footings resting on sand. They reported that the behavior of an eccentrically loaded ring footing was significantly improved with an increase in depth and relative density of the replaced compacted sand layer. Furthermore, Boushehrian and Hataf [18] focused on the behavior of circular footing on sand and reported that the circular foundation was more suitable and economical for axi-symmetric structures. Taiebat and Carter [19, 20] suggested the shape of the failure in (V, H, M) space using the results of a finite element study for circular foundations on undrained clay subjected to eccentric loads where V and H are vertical and horizontal loads and M is the moment applied to the foundation. They claimed that the effective width method commonly used in the analysis of foundations provided good approximations to the collapse loads.

Few studies have been performed for analyzing of the circular footing under eccentric loading. The experimental studies explained above focused on eccentrically loaded strip footing on reinforced soil and no previous study has so far investigated the behaviour of eccentrically loaded circular and square foundation resting on reinforced sand. Thus, prediction of the eccentric bearing capacity circular and square footings with varying number of reinforcement layers is still a challenging subject in foundation engineering. In this sense, in this paper the behavior of a circular and square foundation on unreinforced and reinforced sand under central and eccentric loading are studied and the effect of load eccentricities on rotation of footing and ultimate bearing capacity is presented. Hence, new equations are proposed for reinforced and unreinforced condition to determine the ultimate bearing capacity under eccentric loadings. In this work, many sets of foundation loading data extracted from nine published works, are processed and analyzed. Since the aim of the research is to verify the prediction of proposed method on the behaviour of eccentric loading of reinforced sand, the raw data have been picked from the works that have reported the bearing capacity data at different sand and reinforcement condition. Also the details of the processed datasets are summarized in each analysis. Besides, the proposed equations have been compared in unreinforced conditions with the Effective Area Method proposed by Meyerhof [21] for the evaluation of the previously published laboratory model test results and numerical analyses in the literature review. Finally, the large-scale (field) and laboratory tests results of Saran et al. [15, 16] have been used for validating the

eccentric ultimate bearing capacity, which indicate the accuracy of the proposed method, too.

Eccentric Loadings Background

Meyerhof [21] studied behavior of rectangular footing with eccentric loading and suggested the semi-empirical concept of effective width that can be used to estimate the ultimate bearing capacity of a shallow foundation subjected to one-way load eccentricity. He assumed that the contact pressure of footing decreases linearly from toe to heel, when subjected to a loading with eccentricity. According to this, the bearing capacity of a strip foundation (with width B) can be determined assuming that the load acts centrally along the effective contact width ($B' = B - 2e$) as shown in Fig. 1a where e is load eccentricity. Prakash and Saran [22] provided a comprehensive mathematical formulation to estimate the ultimate bearing capacity and settlement

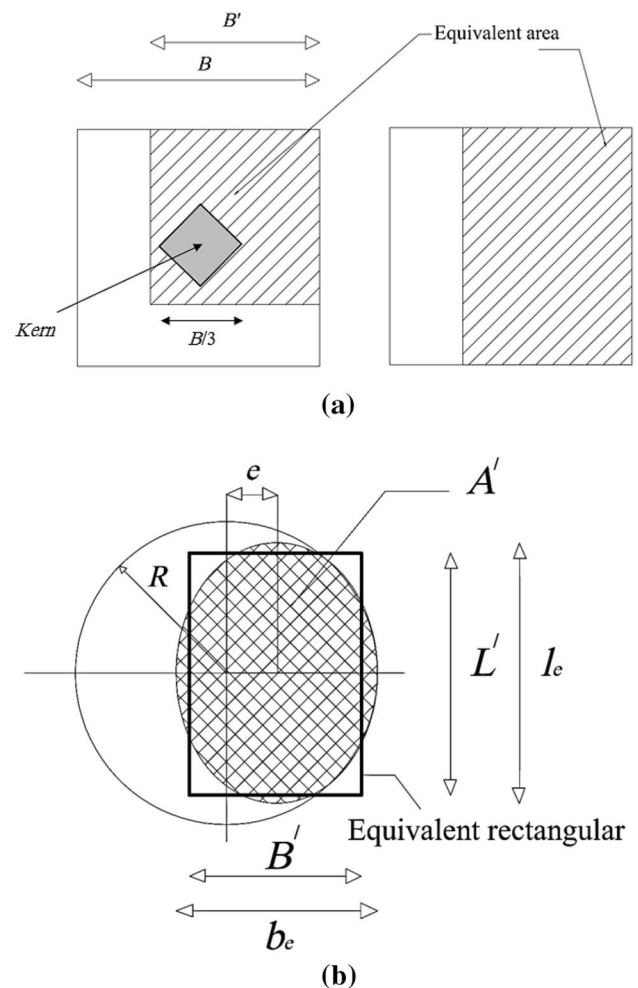


Fig. 1 Effective area method for **a** square section in one-way eccentricity and **b** circular section

for strip foundations in a $c-\phi$ soil subjected to eccentric loading. It was concluded that, for high silos, refinery towers, wind turbines and chimneys, the circular foundation was more economical than any other form of footing, because the direction of wind and earthquake overturning moments were not fixed; and moreover, the load eccentricity is always one-way. In case of circular foundations under eccentric loading, Highter and Anders [23] suggested non-dimensional curves for calculation the effective area A' and the effective width B' . Effective area was defined as the equivalent area of footing, which can be loaded centrally when a vertical load was applied on a location other than the centroid of footing or when a foundation was subjected to a centric load and momentum. Similarly, in this case, Taiebat and Carter [20] suggested that the area of the fictitious foundation, A' , can be calculated using Eq. 1. The width (b_e) and length (l_e) of effective equivalent rectangular are shown in Fig. 1b that can also be determined by Eqs. 2 and 3, respectively.

$$A' = l_e \cdot b_e = \frac{\pi R^2}{4} - \frac{1}{2} \left[e(R^2 - e^2)^{0.5} + R^2 \sin^{-1} \left(\frac{e}{R} \right) \right] \quad (1)$$

$$l_e = \left[A' \left(\frac{R+e}{R-e} \right)^{0.5} \right]^{0.5} \quad (2)$$

$$b_e = l_e \left(\frac{R-e}{R+e} \right)^{0.5} \quad (3)$$

where R is the footing radius, e is the load eccentricity, l_e and b_e are length and width of effective area, respectively. It is well shown by many researchers that for strip and rectangular foundations the effective area method of Meyerhof [21] is an appropriate method for calculating the ultimate bearing capacity of eccentrically loaded foundations. However, many methods have been developed by researchers for the investigation of circular footings under eccentrically loading situations. For instance, Purkayastha and Char [24] carried out stability analyses on eccentrically loaded continuous foundations supported by sand using the slices method proposed by Janbu [25]. Slices method which is the most common limit equilibrium technique, discretized the soil mass into horizontal or vertical slices. They assumed that failure surface under strip footing subjected to eccentrically loading develops to the side of the eccentricity away from the footing. Based on their analysis, they found that the bearing capacity of strip foundation under eccentric loadings was a coefficient of centric bearing capacity of foundation and proposed a reduction factor (R_k) as Eq. 4:

$$R_k = 1 - \frac{q_{u(eccentric)}}{q_{u(centric)}} \quad (4)$$

where R_k is the reduction factor, $q_{u(eccentric)}$ is the ultimate bearing capacity of eccentrically loaded and $q_{u(centric)}$ is the ultimate bearing capacity of centrally loaded footing. Based on a statistical analysis, it was also shown that internal friction angle (ϕ) have not any influence on R_k [2]. The magnitude of R_k can be expressed for shallow foundation with embedment depth of footing equal zero ($D_f = 0$) as Eq. 5:

$$R_k = 1.862 \left(\frac{e}{B} \right)^{0.73} \quad (5)$$

Also, based on the reduction curves of Meyerhof, the following equation is proposed by Bowles [26] for obtaining the reduction factor for footing under eccentric loading resting on non-cohesive soil and for $0 < e/B < 0.3$ as Eq. 6:

$$R_k = \sqrt{\frac{e}{B}} \quad (6)$$

where e is the loading eccentricity and B is the width of footing. It reported that for circular footing B is the diameter of footing. It is worthy to note that the reduction factor proposed by Purkayastha and Char [24] provides larger values than Bowles [26]. Also, it is should be mentioned that the difference between two equations increases with the increment of load eccentricity.

Test Materials and Setup

Sand

The used soil in this investigation includes uniformly graded sand with effective size $D_{10} = 0.18$ mm, coefficient of uniformity $C_u = 10.55$ and coefficient of curvature $C_c = 4.21$ and is classified as *SP* (poorly graded). The grain size distribution curve is determined by dry sieve analysis method on three sand specimens. The average particles

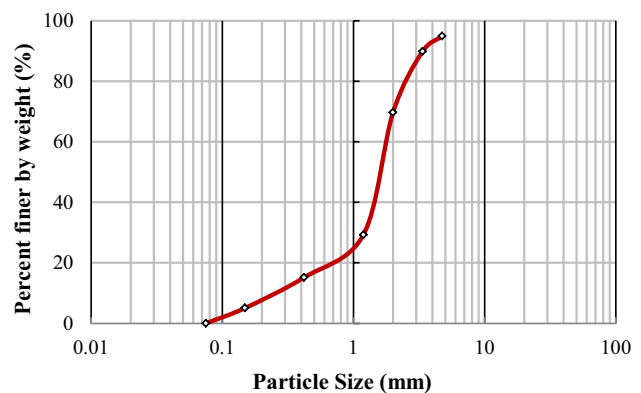


Fig. 2 Particle size distribution curve of sandy soil

size distribution curve is illustrated in Fig. 2. On representative sand specimens, laboratory tests were conducted to determine specific gravity, maximum and minimum dry densities, and direct shear tests under normal stress ranging between 40 and 160 kPa in relative density of 60%. The sand properties are given in Table 1.

Geogrid

In order to provide reinforcement material for the model test, geogrid with tensile strength 7.68 kN/m was used. This reinforcement is made of high density polyethylene (HDPE). The main reason for selecting this type of geogrid was the same peak tensile strength in every direction. The properties of reinforcement layers are given in Table 2.

Laboratory Model Tests

The size of the used tank for conducting the model tests was decided based on the sizes of footings and the influenced zoning. As the Fig. 3 the test tank has inside dimensions of 600 mm \times 600 mm in plan and 600 mm in height. The tank is made from Plexiglas, which is supported directly on two steel beams. To record the footing settlement, a LVDT (Linear Variable Differential Transducer) with 25 mm travel range and 0.001 mm accuracy is utilized. In tests with eccentricity load, two LVDTs are used to measure tilt of the footing. The first LVDT was placed on the footing center and the second LVDT was located at the loading point. The tests were conducted in a controlled strain condition. During the tests, a data logger and a computer was used to record the load and settlements. The used model footings in the present tests were circular with 120 mm in diameter and square with 120 mm in width, which are made of rigid steel plates. Bottom of the models were became rough by a layer of geonet that was fixed with epoxy glue to ensure that the rough condition was same as in the all tests. Diameter of the circular footing was selected <0.2 tank width to ensure that failure planes under footing would be within the tank limit. When the load was applied within a limited

Table 1 Sand properties used in tests

Parameter	Value
Maximum unit weight (kN/m^3)	16.4
Minimum unit weight (kN/m^3)	14.4
Maximum void ratio	0.890
Minimum void ratio	0.658
Specific gravity	2.65
Average dry unit weight (kN/m^3) at $D_r = 60\%$	15.64
Internal friction angle ($^\circ$)	39

Table 2 The engineering properties of the geogrid used in the tests

Property	Value
Polymer type	Polyethylene
Tensile strength (kN/m)	7.68
Extension at 1/2 peak load (%)	1.61
Tensile strength at 10% extension (kN/m)	0.96
Weight (g/m^2)	730
Ultimate tensile strength (kN/m)	7.68
Failure strain (%)	4
Secant modulus at 4% strain (kN/m)	219

area which is known as *Kern* rhombic [23], a maximum pressure occurs at the corners or edges of the footing and minimum pressure becomes zero. *Kern* boundary is $R/4$ for circular foundation. In a loading inside the *Kern* boundary, whole footing area is under pressure. Outside the *Kern* boundary, the footing edge is subjected to uplift pressure. The loading on the *Kern* boundary caused that the edge pressure becomes zero. In this study, five different load eccentricities are selected: $e/D = 0.0417$ and 0.0833 for inside the *Kern* boundary, 0.125 for on the *Kern* boundary, and 0.1667 and 0.2083 for outside the *Kern* boundary. The load eccentricities can be located on the model footing by small holes. Also, five different load eccentricities are considered, in one-way and two-ways namely, for the square footing: $e = 0.5, 1, 1.5, 2$ and 2.5 cm equal to $e/B = 0.0417, 0.0833, 0.125, 0.1667$ and 0.2083 .

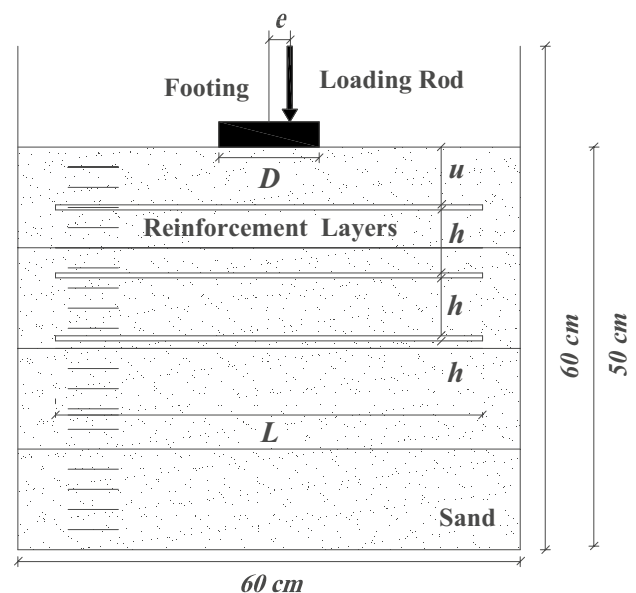


Fig. 3 Geometric parameters studied in the laboratory model tests

Experimental Program

In order to provide experimental control and repeatability of the tests, the sandy soil was placed in the tank using raining technique. The height of raining to achieve the desired density was determined by performing a series of trials with different heights of raining. Then, sand was rained from 40 cm height to maintain a stable relative density of 60% in all the tests. By placing a metal cup in different heights in the tank, the relative density of sand is monitored, too. After preparing the tank soil up to 50 cm height, the surface of sand is leveled by special ruler. Later on, the footing is placed on the sand and the rate of displacement sets at 1 mm/min. In the reinforced cases a square shaped geogrid layer, 4.5 times the diameter of footing ($L/D=L/B=4.5$) with depth ratios of $u/D=u/B=0.42$ and $h/D=h/B=0.42$ based on researches [27–32] was placed after leveling the surface of the sand and pouring was continued to the selected surface of footing.

Results of Experimental Models

The results include of load-settlement curves from 68 experimental tests which are carried out on centrally and eccentrically loaded circular and square footings in both reinforced and unreinforced conditions are presented in this section. For both loading the number of geogrid layers is increased from 1 to 3. Several tests are repeated twice to verify the repeatability and consistency of the test result and the average of each of two tests are considered. It should be noted that the difference between load-settlement curves are less than 4% by the same load-displacement patterns. The load-settlement curves of circular and square footings under various load eccentricity are illustrated in Fig. 4. As expected, when the load eccentricity increases, the ultimate load decreases. In addition, by increasing the load eccentricities, the settlement at maximum load (i.e. vertical displacement values at failure) decreases for both circular and square footings. The ultimate loads of foundation for centrally and eccentrically loading are obtained from the curves of load-settlement according to suggestions of Boushehrian and Hataf [18] and Sawwaf and Nazir [17]. In all the tests, two LVDTs are used to record the settlement of footing at two points. Footing tilt is calculated to be the difference ratio of two LVDTs to the distance between them. The ultimate loads at centrally and eccentrically loadings for unreinforced and one, two and three layers of reinforcement are displayed in Tables 3, 4, 5 and 6. The efficacy of reinforcement in increasing the ultimate load is expressed as a non-dimensional quantity called the Improvement Index, which is defined as the ratio of ultimate load of reinforced soil to ultimate load of unreinforced

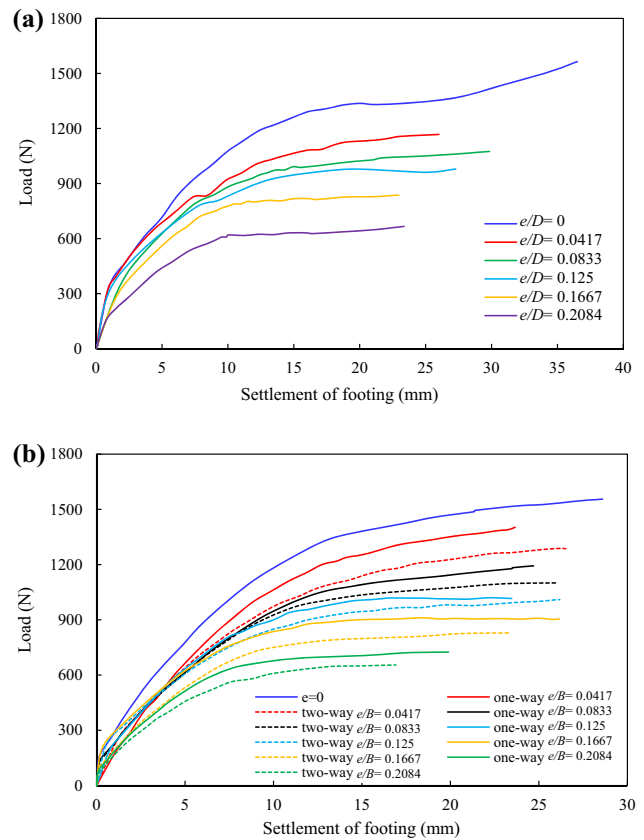


Fig. 4 Load-settlement curves for various load eccentricities, **a** circular and **b** square footing

Table 3 Ultimate load for unreinforced condition

e/D or e/B	Ultimate load of footing (N)		
	Circular	Square	
		One-way	Two-ways
0.0	1318	1492	1492
0.0417	1192	1359	1256
0.0833	1046	1165	1103
0.1250	936	1049	964
0.1667	816	889	834
0.2083	614	680	649

soil. Improvement Index increases with increase of number of reinforcement layers for all the tests, but the improvement is more significant for circular footing. Also, by increasing the load eccentricity, reinforcement layers have more influence on circular footing than square footing.

When the load is transmitted at the base of footing the moment of the soil particles in horizontal and vertical direction occurs. Due to eccentric loading the footing tilt and pressure below the footing does not remain uniform.

Table 4 Ultimate load for one layer of reinforcement

e/D or e/B	Ultimate load of footing (N)			Improvement index ($q_{u(\text{reinforced})}/q_{u(\text{unreinforced})}$)		
	Circular	Square		Circular	Square	
		One-way	Two-ways		One-way	Two-ways
0.0	2892	2292		2.19	1.54	1.54
0.0417	2662	2025	1980	2.23	1.49	1.58
0.0833	2552	1890	1670	2.44	1.62	1.51
0.1250	2380	1560	1430	2.54	1.60	1.48
0.1667	2250	1330	1159	2.76	1.64	1.39
0.2083	1988	1201	984	3.24	1.83	1.52

Table 5 Ultimate load for two layers of reinforcement

e/D or e/B	Ultimate load of footing (N)			Improvement index ($q_{u(\text{reinforced})}/q_{u(\text{unreinforced})}$)		
	Circular	Square		Circular	Square	
		One-way	Two-ways		One-way	Two-ways
0.0	4415	3202		3.35	2.15	2.15
0.0417	4020	2800	2746	3.34	2.06	2.19
0.0833	3710	2540	2280	3.59	2.18	2.07
0.1250	3518	2189	1860	3.76	2.09	1.93
0.1667	3150	1801	1462	3.81	2.03	1.75
0.2083	2901	1595	1101	4.22	2.35	1.84

Table 6 Ultimate load for three layers of reinforcement

e/D or e/B	Ultimate load of footing (N)			Improvement index ($q_{u(\text{reinforced})}/q_{u(\text{unreinforced})}$)		
	Circular	Square		Circular	Square	
		One-way	Two-ways		One-way	Two-ways
0.0	5450	4120		4.19	2.76	2.76
0.0417	4980	3562	3427	4.18	2.64	2.78
0.0833	4435	3111	2893	4.24	2.74	2.63
0.1250	4120	2789	2467	4.40	2.55	2.27
0.1667	3680	2140	1894	4.51	2.62	1.98
0.2083	3126	1688	1205	5.25	2.56	1.95

The edge near to the load settles more than the other edge. Thus two edges of the footing settle by different amount that causes rotation of footing. The tilt will occur in a direction in which the settlement is higher. The amount of tilt and the pressure at the base depends upon the value of eccentricity width ratio. Footing tilt curves (in degree) at ultimate load versus load eccentricities for both footings are presented in Fig. 5. When eccentricity to width or diameter ratio (e/B or e/D) is greater than the *Kern* boundary, the edge of the footing away from load will lose its contact with the soil which will result in the reduction of effective width of footing and hence reduction of ultimate load of foundation. For circular footing, when load eccentricity is outside the *Kern* of footing the rate of increment affects larger than inside the *Kern*

in comparison with square footing for both one-way and two-ways load eccentricities. Using of the reinforcement layers the tilt of footing decreases in comparison with the unreinforced tests for both footings, but the reinforcement layers has more influence on circular footing than square footing. The tilt of footing increases with increment of load eccentricity and the footing rotation increases linearly with increment of displacement as shown in Fig. 6, that investigated the effects of different settlements on footing rotation in reinforced sand with three layers of geogrid at the same load eccentricity. The main reason for the lower tilt of the circular footing in comparison with square footing in reinforced condition may be attributed to reinforcement mechanism which limits the spreading and lateral deformations of

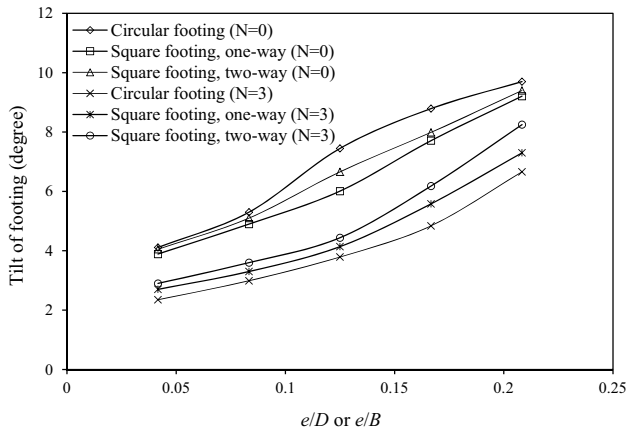


Fig. 5 Tilt of footing versus load eccentricity

sand. The circular footing causes a bigger mobilized tension in reinforcement layers that enables the reinforcement to resist the imposed horizontal shear stresses built up in the mass beneath the loaded area by transferring the footing load to deeper layers of soil. Therefore, the failure wedge becomes larger and the frictional resistance on failure planes becomes greater.

Proposed Method for Prediction of Eccentric Ultimate Bearing Capacity

Unreinforced Sand

It is appear that the presented ultimate bearing capacities in Table 3 can be expressed in a form similar to those proposed by Purkayastha and Char [24] as reduction factors. With regard to data sets, a curved line is used to graphically display trend in average data to help predicting of reduction

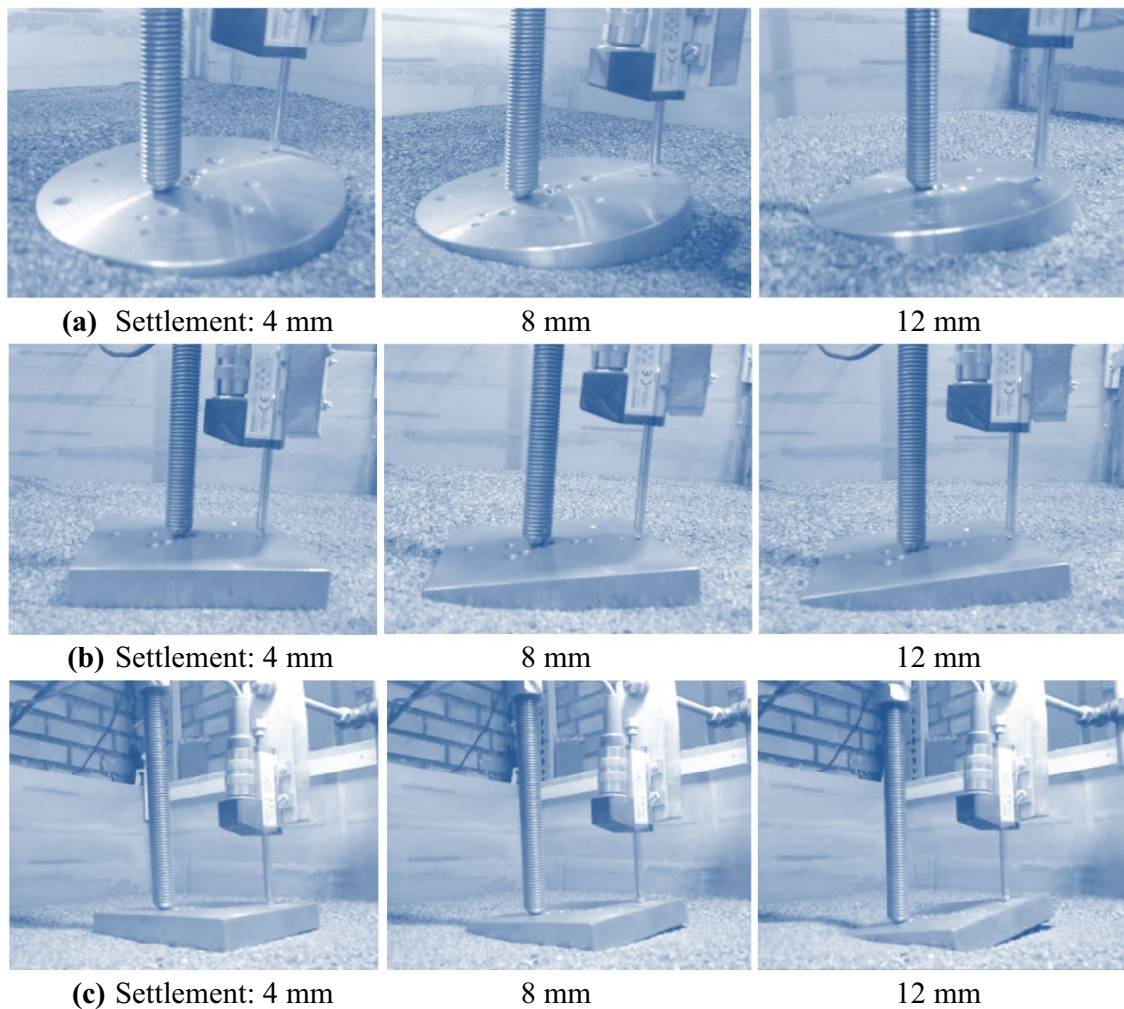


Fig. 6 Settlement and footing rotation for different footing on reinforced with three layers for a circular, b square one-way and c square two-way

factors in this condition. Based on the increase of measurements at a specific rate a power trend line is considered. New reduction factor is proposed based on the trend line from test results for shallow (embedment depth of zero) circular and square foundations under eccentric loading as given in Eq. 7 for unreinforced condition, where e is the load eccentricity and D or B is the circular footing diameter or width of square footing.

$$q_{u(e)} = q_{u(e=0)}(1 - R_k) = q_{u(e=0)} - q_{u(e=0)} \times \alpha \left(\frac{e}{B \text{ or } D} \right)^k \tag{7}$$

The reduction factors (R_k) versus load eccentricity for both footings are presented in Fig. 7. Based on this figure it is obvious that the rates of increase in R_k have the same behavior for the both of footings (circular and square footings) under different load eccentricities. For R_k , average values of each footing are taken for the plot of the results graph. The average values of α and k are 2.313 and 0.945, respectively. The experimental reduction factor increases by increasing the load eccentricity ratio. To verify the proposed formulation, the reported experimental or numerical results in several investigations [33–37] are compared with the calculated bearing capacities of Meyerhof’s method and the proposed reduction factor. The details of the processed datasets and comparison between the measured and estimated bearing capacities for the circular and square footings on unreinforced sand are summarized in Table 7. The ultimate bearing capacity equation of Meyerhof [21] for non-cohesive soils on shallow footing can be expressed by $q_u = 0.5B'\gamma N_\gamma \lambda_{\gamma s}$, where q_u is the ultimate bearing capacity per unit area of the footing effective surface, B' is the effective width of the footing, γ is the effective soil unit weight and N_γ and $\lambda_{\gamma s}$ are respectively the bearing capacity factor and shape factor which are defined in Eqs. 8 and 9, where for circular and square footing $B = L = D$.

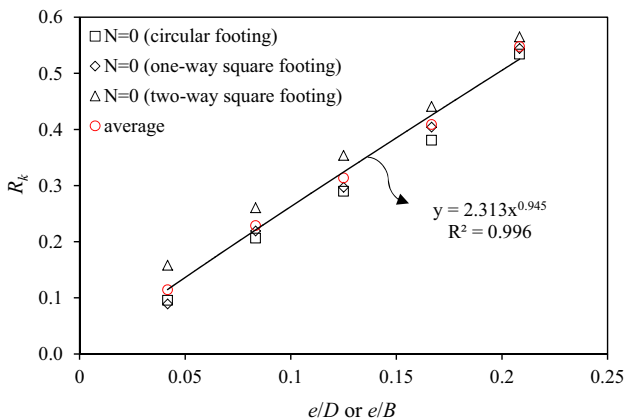


Fig. 7 Reduction factor versus load eccentricity

$$N_\gamma = [2.72^{\pi \tan \phi} \left(\frac{1 + \sin \phi}{1 - \sin \phi} \right) - 1] \tan(1.4\phi) \tag{8}$$

$$\lambda_{\gamma s} = 1 + 0.1 \left(\frac{B}{L} \right) \tan^2 \left(45 + \frac{\phi}{2} \right) \tag{9}$$

According to the presented error in Table 7, it is evident that the predicted values by using the effective area of Meyerhof’s method and the proposed formulation are in good agreement with experimental or numerical results for both footings in terms of eccentric ultimate bearing capacity. For some models, the difference between the ultimate bearing capacity (q_u) and that in the proposed method is lesser than effective area of Meyerhof. It can be seen from Table 7 that the effective width concept generally overestimated the performance of unreinforced sand. However, the predicted ultimate bearing capacity values with the proposed method have a maximum error less than Meyerhof’s method. It is worth to note that, based on this investigation, one can find that increasing of the footing diameter or footing width (D or B) and internal friction angle (ϕ) have not any influence on the reduction factor which has been also reported by Purkayastha and Char [24] and Patra et al. [2].

Reinforced Sand

Based on the laboratory results, a solution for estimating the eccentric ultimate bearing capacity of geogrid reinforced sand for the both of footings in one-way and two-way load eccentricities are developed. As Eq. 4, R_k is defined as Eq. 10, where $q_{u(eccentric, reinforced)}$ is the eccentric ultimate bearing capacity of reinforced soil foundation and $q_{u(centric, unreinforced)}$ is the centric ultimate bearing capacity of unreinforced soil foundation.

$$R_k = 1 - \frac{q_{u(eccentric, reinforced)}}{q_{u(centric, unreinforced)}} \tag{10}$$

It is worth to note, the advantage of the proposed method in reinforced condition is that eccentric ultimate bearing capacity in reinforced sand predicts from centric ultimate bearing capacity in unreinforced sand which is well known by many researchers and can be predicted simply with theoretical methods. As reduction factor in reinforced sand may contain negative values and cannot create an exponential trend line, therefore a constant value (π) is added to the R_k . A non-linear regression model is utilized to illustrate the increasing amount of reduction factor values in an object as it loaded eccentrically. The linear relationship lead to the nearly linear increase of reduction factor with the increase of number of reinforcement layers, and no convergence can be obtained, while the proposed power best fit relations overcomes this shortcoming and converges as the number

Table 7 Measured versus estimated bearing capacities on unreinforced sand

Source work	γ (kN/m ³)	ϕ (°)	Footing	D or B (mm)	Method	e/B or e/D	q_u (kPa)	Error (%)			
								Measured	Proposed method	Meyerhof method [21]	Meyerhof method [21]
Richard et al. [38]	15.40	33	Square	400	Experimental	0.125	120	126	139	5.0	15.8
	15.40	34	Square	400	Experimental	0.125	138	146	159	5.8	15.2
	15.40	35	Square	400	Experimental	0.125	160	163	180	1.9	12.5
Foundoukos and Jardine [37]	16.70	35	Circular	50	Experimental	0.10	33	30	17	-9.1	-48.5
	16.70	35	Circular	50	Experimental	0.20	27	20	15	-25.9	-44.4
	16.70	35	Circular	50	Experimental	0.30	23	11	13	-52.2	-43.5
	16.70	35	Square	50	Experimental	0.10	30	30	17	0.0	-43.3
	16.70	35	Square	50	Experimental	0.20	25	20	13	-52.0	-48.0
Singh et al. [35]	16.70	35	Square	50	Experimental	0.30	21	11	9	-47.6	-57.1
	14.78	34	Square	150	Experimental	0.10	88	99	38	12.5	-56.8
	14.78	34	Square	150	Experimental	0.20	57	66	28	15.8	-50.9
Sahoo [33]	14.78	34	Square	150	Experimental	0.30	29	34	19	17.2	-34.5
	14.36	40.8	Square	100	Experimental	0.05	102	104	103	2.0	1.0
	14.36	40.8	Square	100	Experimental	0.10	78	89	91	14.1	16.7
Dhar et al. [34]	14.36	40.8	Square	100	Experimental	0.15	65	74	80	13.8	23.1
	14.31	39	Square	175	Experimental	0.125	93	84	104	-9.7	12.9
	14.31	39	Square	175	Experimental	0.17	81	73	92	-9.9	13.6
Shen et al. [36] ^a	15.50	38	Circular	250	Numerical	0.10	0.76 $q_{(e=0)} = 134$	131	139	-2.2	3.7
	15.50	38	Circular	250	Numerical	0.15	0.64 $q_{(e=0)} = 113$	109	130	-3.5	15.0
	15.50	38	Circular	250	Numerical	0.20	0.52 $q_{(e=0)} = 92$	88	122	-4.3	32.6
	15.50	38	Circular	250	Numerical	0.25	0.39 $q_{(e=0)} = 69$	67	113	-2.9	63.8
	15.50	38	Circular	250	Numerical	0.30	0.32 $q_{(e=0)} = 56$	46	105	-17.9	87.5

^aNormalised eccentric bearing capacity of foundation ($q_u/q_{(e=0)}$) is reported

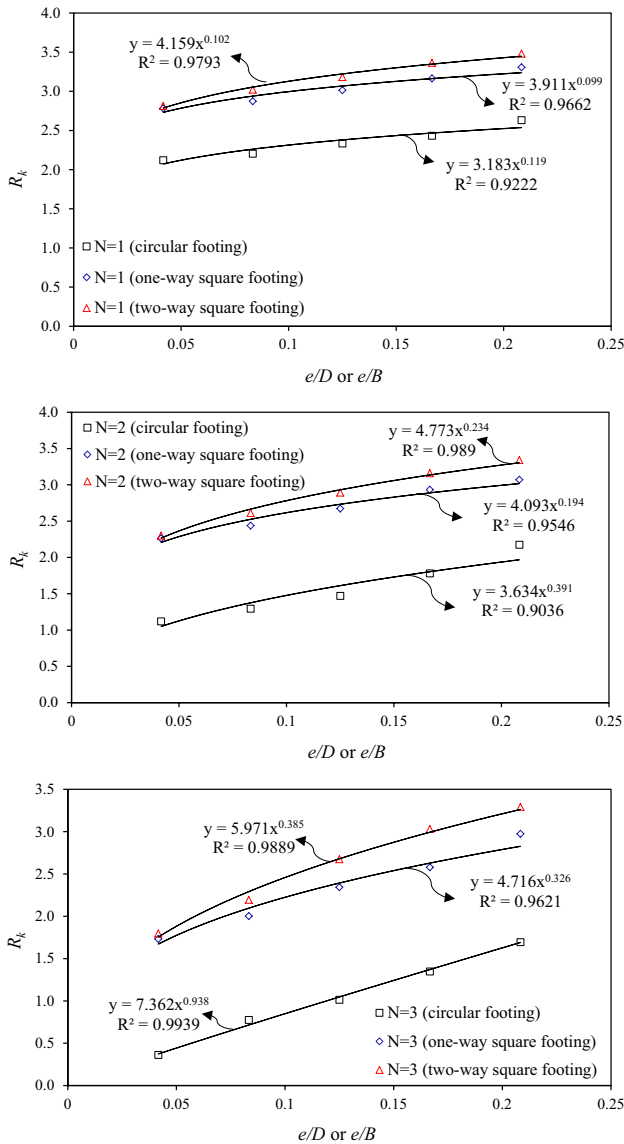


Fig. 8 Reduction factor versus load eccentricity in reinforced condition

of reinforcement layers increases. This exponential trend line is based on the Eq. 11:

$$R_k = \alpha' \left(\frac{e}{B \text{ or } D} \right)^{k'} \quad (11)$$

where the α' and k' are constants. The experimental values of R_k versus different load eccentricities for every number of reinforcement layers are given in Fig. 8. As demonstrated in this figure, in contrast to unreinforced sand, circular and square footings result different values of R_k in the same test condition. It is worth to note that the R -squared values are larger than 0.95, meaning that the lines fit the data perfectly. The circular footings have a lower value of reduction in comparison with square footings. Besides, for

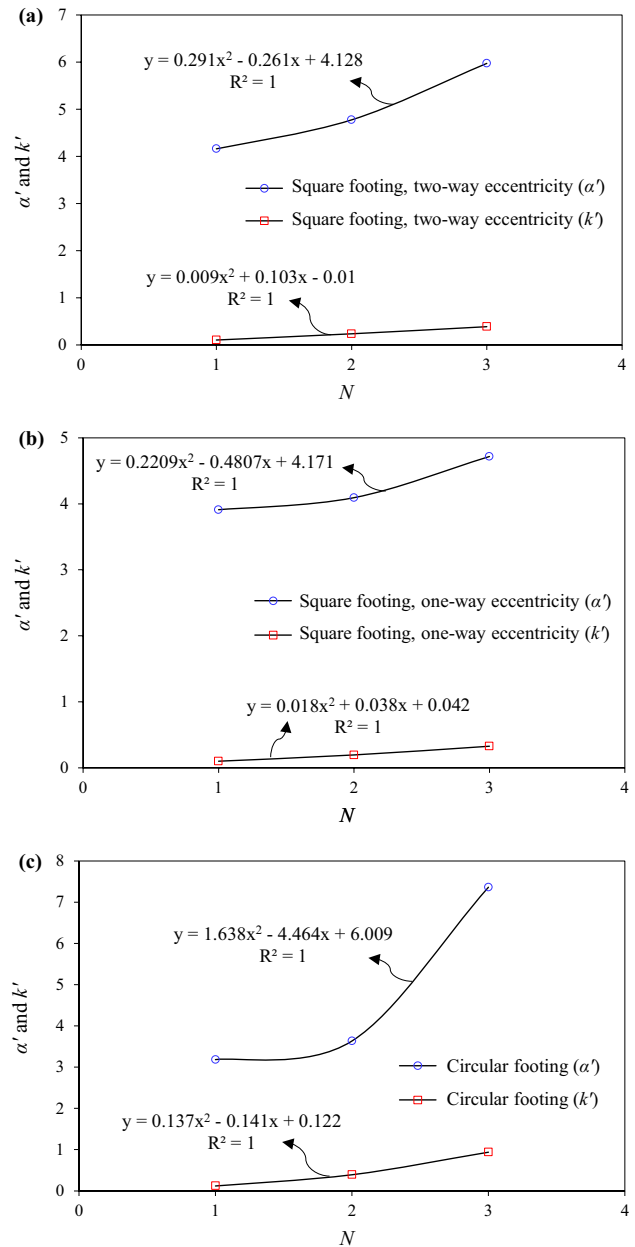


Fig. 9 Values of α' and k' versus the number of reinforcement layers, **a** square footing with two-way load eccentricity, **b** square footing with one-way load eccentricity and **c** circular footing

square footing, two-way eccentricities demonstrated higher reduction to one-way eccentricities. While, by increasing the load eccentricity the difference between related reduction factors becomes more with an almost linear increment. The new bearing capacity formula (Eq. 12) that incorporated the contribution of reinforcements to the increase in eccentrically bearing capacity is developed as follow for both type of footing:

$$q_{u(eccentric, reinforced)} = q_{u(centric, unreinforced)} \times (1 + \pi - R_k) \quad (12)$$

The values of α' and k' versus the number of reinforcement layers for circular, square with one-way and two-way eccentricity are shown in Fig. 9. An order of two polynomial trend lines is used to predict influence of N on the values of R_k for circular and square footings with one-way and two-way load eccentricities, respectively. Results show the R -squared values for them are one, which indicate acceptable fit of the lines to the data. The parameters of reduction factor can be easily evaluated with these equations to determine the ultimate bearing capacity on reinforced sand. A comparison is made between large-scale work of Saran et al. [15] and the proposed method for square footing width $B = 1000$ mm and load eccentricities of $0.1 B$ placed at a depth zero below the ground level in reinforced condition which is shown in Table 8. The unit weight of sand was 15 kN/m^3 and angle of internal friction was 35° . The used geogrid in model tests had tensile strength 20 kN/m at 5% strain in both the machines and the cross-machine directions and sand-geogrid frictional angle was 22° . Also the proposed solutions are verified by the results of laboratory model tests conducted by Badakhshan and Noorzad [2] for circular footing on geogrid-reinforced sand under eccentric loadings with reinforcement tensile strength 7.68 kN/m at 2.5% strain. It is clear that the predicted values by using the proposed solution are in good agreement with those obtained in model test results of Saran et al. [15] and Badakhshan and Noorzad [39]. In order to ensure the capability of the proposed equations, the obtained test results by Saran et al. [16] on square footing subjected to one-way eccentric load resting on reinforced sand, are also compared with the calculated bearing capacities. The related test soil is classified as poorly graded sand (SP) and physical properties of test sand such as maximum void ratio (e_{\max}), minimum void ratio (e_{\min}), relative density are determined as 0.913 , 0.509 and 65% , respectively. The unit weight of sand is about of 16.0 kN/m^3 . The angle of internal friction is obtained from triaxial tests about 39° . Tensor SS20 geogrid was used to reinforce the sand throughout the model test program. The tensile strength of geogrid both in the longitudinal and transverse directions is equal to 20 kN/m . The square footing measures $200 \text{ mm} \times 200 \text{ mm}$ in plan. Depth of the top-most layer (u) and vertical spacing between adjacent layers of reinforcement (h) were kept as $0.25B$, where, B is the width of the footing. Size of each reinforcement layers (L_r) was taken as B , $2B$ and $3B$. These tests were conducted on the footing for $e/B = 0.1$ and 0.2 . It can be seen from Table 8 that the proposed method are in good agreement with the test results of Saran et al. [16] in tests with L_r bigger than two. It is worth to note, the advantage of the proposed method in reinforced condition is that eccentric ultimate bearing capacity in reinforced sand predicts from centric ultimate bearing capacity in unreinforced sand which is well known by many researchers and

can be predicted simply. Also, as in experimental tests that conducted by the authors, based on previous researches [27–32] the optimum length of reinforcement is selected $L_r = 4.5B$, and the proposed equation is compatible with this condition and in others un-optimum lengths such as some of the test results of Saran et al. [16], the proposed equation has an unacceptable error. On the other hands, the proposed method provided a good prediction of eccentric ultimate bearing capacity for models with a maximum error less than 14% in optimum condition of reinforced soil.

Finite Element Procedure

Numerical analysis based on finite element method (FEM) in a three-dimensional space is provided for two purposes as verifying the laboratory tests conducted by the authors and studying the behavior of reinforcement layers. The constructed numerical model is validated using experimental data obtained for circular footing on three layers of reinforcement in load eccentricity $e/D = 0.125$. Essential and geometric boundary conditions which were prescribed displacement equal to zero at the boundary of the simulation domain are utilized in modeling. Thus, supports were used to restrain foundation soil bed boundaries against relative rigid body motions. For the modeling, boundary conditions were chosen such that nodes at the base of the model are restricted in all directions (full fixity of displacement in both directions x and y), while vertical boundaries were restricted horizontally (fixity of displacement in directions x) and were free to move in the vertical direction. The properties of sand and reinforcement layers were chosen such that those used in the laboratory test. A first step towards accurate modeling of geosynthetic was choosing a suitable material model. In previous works the only material property of reinforcement was elastic normal (axial) stiffness but in the current study the reinforcement layers are modeled as a linear elastic material. The soil was discretized using 10-noded tetrahedron solid elements while the reinforcement was modeled with 4-noded rectangular membrane elements which having negligible bending stiffness. Membrane elements were used to represent thin surfaces in space that offer strength in the plane of the element but have no bending stiffness. The thickness of reinforcement layer was assumed 4 mm in all models as actual condition. Secant modulus of elasticity for the reinforcement per unit length which chosen from the manufacturer's manual is about 219 kN/m . Also analysis was performed under displacement control. In modeling the yielding of frictional material (sand), the elastic-perfectly plastic Drucker–Prager constitutive model with a non-associated flow rule was used. The parameters adopted for the analysis are given in Table 9. The parameters (d) and (β) are the cohesion and

Table 8 Measured versus estimated bearing capacities on reinforced sand

Source work	Tensile strength of reinforcement (kN/m)	γ (kN/m ³)	ϕ (°)	N	Footing	B (mm)	Method	e/B	u/B	h/B	L _r	q _u (kPa)		Error (%)
												Measured	Proposed method	
Saran et al. [15]	20	15	35	1	Square	1000	Large-scale	0.1	0.25	-	4	530	526	6.07
	20	15	35	2	Square	1000	Large-scale	0.1	0.25	0.25	4	990	1011	-2.12
	20	15	35	3	Square	1000	Large-scale	0.1	0.25	0.25	4	1533	1444	5.81
Badakhshan and Noorzad [39]	7.68	15.14	39	1	Circular	120	Laboratory	0.125	0.42	-	4.5	223	193	13.45
	7.68	15.14	39	2	Circular	120	Laboratory	0.125	0.42	0.42	4.5	317	294	7.26
	7.68	15.14	39	3	Circular	120	Laboratory	0.125	0.42	0.42	4.5	371	359	3.23
Saran et al. [16]	20	16	39	2	Square	200	Laboratory	0.1	0.25	0.25	2	235	187	-25.67
	20	16	39	3	Square	200	Laboratory	0.1	0.25	0.25	2	300	237	-26.58
	20	16	39	4	Square	200	Laboratory	0.1	0.25	0.25	2	375	314	-19.43
	20	16	39	1	Square	200	Laboratory	0.1	0.25	0.25	3	210	231	9.09
	20	16	39	2	Square	200	Laboratory	0.1	0.25	0.25	3	265	244	-8.61
	20	16	39	3	Square	200	Laboratory	0.1	0.25	0.25	3	324	309	-4.85
	20	16	39	4	Square	200	Laboratory	0.1	0.25	0.25	3	415	371	-11.86
	20	16	39	4	Square	200	Laboratory	0.2	0.25	0.25	1	216	299	27.76
	20	16	39	4	Square	200	Laboratory	0.2	0.25	0.25	2	288	315	8.57
20	16	39	4	Square	200	Laboratory	0.2	0.25	0.25	3	298	323	7.74	

Table 9 Material properties used in numerical models

Characteristics	Value	
	Soil	Reinforcement
Friction angle (°)	39	–
Density (kN/m ³)	14.40	0.0073
Modulus of elasticity (MPa)	40	54.8
Poisson’s ratio	0.30	0.30
Cohesion (kPa)	1	–
Dilatancy (°)	9	–
Flow rule	non-associate	–
β	0.63	–
d (kPa)	0.77	–
Tensile stiffness (kN/m)	–	219
μ	–	0.50
E_{slip}	–	0.005

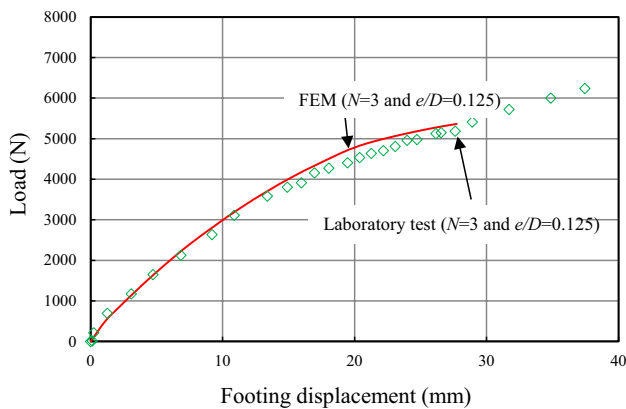


Fig. 10 Validation of laboratory tests for circular footing

internal frictional angle used in the Drucker–Prager constitutive model. More details on these parameters can be found in Helwany [40]. The model was divided into four main domains; the top soil (above the reinforcement), the bottom soil (below the reinforcement), foundation and the reinforcement layers. It is worth to say that a small cohesion value (1 kN/m²) is used in this study to improve the stability of the analyses and avoid any singularity that may arise. The interaction between reinforcement and sand was modeled at both sides by using interface elements. For define interface between the sand (solid elements) and the reinforcement layers (membrane elements) a parametric study is conducted and indicates that using of the surface to surface contact model with the traditional node to surface contact formulation is suitable. It should be noted that the behavior of the soil-reinforcement interface is simulated using the Coulomb friction model with two material parameters such as friction coefficient (μ) and tolerance parameter (E_{slip}). Figure 10 compares the obtained results from

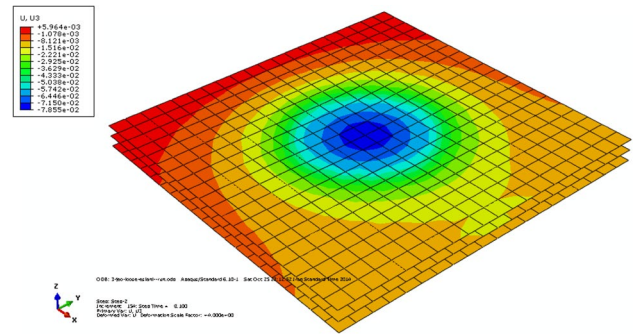


Fig. 11 vertical displacement contours for reinforcement layers

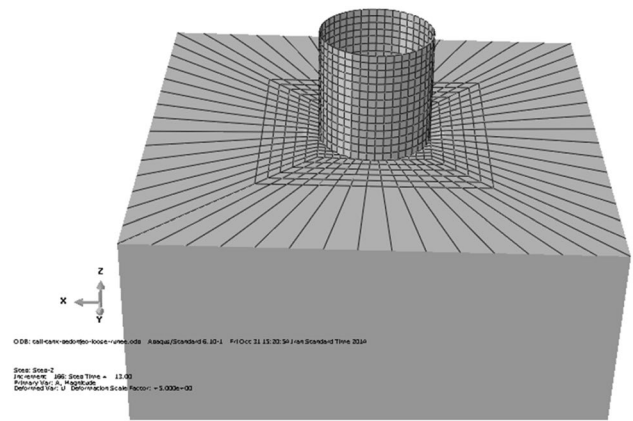


Fig. 12 Finite element mesh for large scale models

the laboratory model test and numerical analysis. As seen, this comparison is satisfactory, thus the results of a larger footing may be determined. Also, the numerical analysis is taken up to understand the reinforcement behavior mechanism further in light of stress and displacement distributions underneath the footings. Vertical displacements contours of embedded reinforcement layers in sand are shown in Fig. 11 from numerical analysis. This figure clearly indicates that the utilized reinforcement layers lengths are appropriate for this analysis. As be expected, the vertical displacement of the upper layer (located closer to the footing) is larger than that of the lower one. Also most of the geogrid deformations occur mainly in the area immediately below the footing with very small deformation away from the loaded area. The comparison between experimental test and numerical model demonstrates that the proposed approach for modeling unconfined geogrid in 3D is suitable for solving geogrid-reinforced soil systems and this agreement can confirm the accuracy of proposed equations. For comparison of the proposed method with a large scale circular footing in reinforced sand with load eccentricity, in numerical analysis of large-scale the diameter of footing is selected 2.5 m. Figure 12 shows 3D finite element mesh

used in this analysis. The sand and reinforcement layers are chosen as same as the above. The results of numerical large scale models are compared with results of current study to find out the ability of the proposed method to calculate eccentric bearing capacity of real scale footing. For this purpose the different load eccentricity ratio ($e/D=0.05, 0.1$ and 0.15) in $N=3$ condition ($u/D=h/D=0.42$) were considered. The ultimate bearing capacity of footing in desired load eccentricities is determined about 6303, 5877 and 4833 kPa for numerical models and calculated about 6798, 6012 and 5262 kPa for proposed method, respectively. Comparison of estimated and numerical values of bearing capacity for the large scale analyses on reinforced sand present that there are very good agreement between measured values with numerical models and proposed methods.

Design Example

It is required to predict the ultimate bearing capacity of a square footing resting on reinforced sand to carry safely, a central load with eccentricity of 0.1. The unit weight of sand is 15 kN/m^3 and angle of internal friction is 35° . The sand below the footing is reinforced with geogrid of 20 kN/m strength. Taking footing of width $B=500 \text{ mm}$, placed at a depth zero below the ground level and sand is reinforced in three layers with $L_r = 4.5$ and embedment depth ration $u/B=h/B=0.42$. In this condition for prediction the ultimate bearing capacity of reinforced sand, at the first time the centric-unreinforced ultimate bearing capacity of footing must be determined by an appropriate theoretical method for example Meyerhof equation. Thus, the value of $q_{u(\text{centric,unreinforced})}$ calculates about 189 kN/m^2 . By using the value of reduction factor related to the $e/B=0.1$ and $N=3$ from Fig. 8, can obtain the ultimate bearing capacity on reinforced sand under one-way eccentric loading based the Eq. 12. In this example the value of R_k calculate about 2.226 and consequently the $q_{u(\text{eccentric,reinforced})}$ determine about 361 kN/m^2 .

Conclusions

The current paper presents obtained data from laboratory tests carried out on shallow circular footing with 120 mm in diameter and square footing of 120 mm in width under central and eccentric loadings resting on unreinforced and reinforced sandy soil. An equation is proposed for eccentrically loaded circular and square footings resting on reinforced sand. The results are in fair agreement with those of Meyerhof's method in unreinforced condition. Also, finite element method (FEM) in a three-dimensional space is used for verifying the laboratory tests and studying the

behavior of reinforcement layers. Based on the obtained results, the following main conclusions were drawn:

1. By increasing the load eccentricity, ultimate bearing capacity decreases and this reduction is more when the load eccentricity is larger than footing *Kern* for both circular and square footings. The footing tilt increases linearly with load eccentricity and this rate for load eccentricities inside the *Kern* is smaller than outside the *Kern*. Also, the tilt of footing at ultimate bearing capacity, from center to *Kern* increase about 18%, but while this increase is about 53% to outside the *Kern*.
2. Improvement Index increases with increase of number of reinforcement layers for all the tests, but the improvement is more significant for circular footing and by increasing the load eccentricity, reinforcement layers have more influence on circular footing than square footing. The circular footing causes a bigger mobilized tension in reinforcement layers that enables the reinforcement to resist the imposed horizontal shear stresses built up in the mass beneath the loaded area by transferring the footing load to deeper layers of soil in comparison with square footing.
3. Based on this method, the eccentrically ultimate bearing capacity for both of circular and square footings can be calculated which is only dependent on the load eccentricity ratio (e/D or e/B) and unreinforced central ultimate bearing capacity.
4. The process of calculating the bearing capacity has been simplified by presenting suitable charts in non-dimensional form that can be directly used for the same purpose. It is shown that the new reduction factor that is capable of predicting the one-way and two-way eccentric ultimate bearing capacity of circular and square footings on geogrid reinforced soil is depended to the two parameters of α' and k' . The measured values by using the proposed solution are compared with the large scale tests and large scale numerical model and show a good agreement with a maximum error less than 14%.

References

1. Sawaf M (2009) Experimental and numerical study of eccentrically loaded strip footings resting on reinforced sand. J Geotech Geoenviron Eng ASCE 135(10):1509–1518
2. Patra CR, Das BM, Bhoi L (2006) Eccentrically loaded strip foundation on geogrid reinforced sand. Geotext Geomembr 24:354–359
3. Sadoglo E, Cure E, Moroglu B (2009) Ultimate loads for eccentrically loaded model shallow strip footings on geotextile reinforced sand. Geotext Geomembr 27:176–182

4. Al-Tirkity J, Al-Taay A (2012) Bearing capacity of eccentrically loaded strip footing on geogrid reinforced sand. *J Eng Sci* 19(1):14–22
5. Sharma R, Chen Q, Abu-Farsakh M (2009) Analytical modeling of geogrid reinforced soil foundation. *Geotext Geomembr* 27:63–72
6. Rahmaninezhad SM, Yasrobi SS, Eftekharzadeh SF (2009) Effects of compaction in the subgrade of the reinforced sand backfills with geotextile on bearing capacity. *Int J Civil Eng* 12:320–328
7. Lovisa J, Kumar S, Sivakugan N (2010) Behavior of pre-stressed geotextile-reinforced sand bed supporting a loaded circular footing. *Geotext Geomembr* 28:23–32
8. Phanikumar BR, Prasad R, Singh A (2009) Compressive load response of geogrid-reinforced fine, medium and coarse sands. *Geotext Geomembr* 27:183–186
9. Verma V, Yadu LK (2014) Response of circular footing by varying the vertical spacing of reinforcement resting on structural fill. *IJIRSET* 3:16294–16299
10. Chakraborty M, Kumar J (2014) Bearing capacity of circular foundations reinforced with geogrid sheets. *Soils Found* 54(4):820–832
11. Michalowski RL (1997) An estimate of the influence of soil weight on bearing capacity using limit analysis. *J Soil Mech Found Eng* 37(4):132–154
12. Michalowski RL (2004) Limit Loads on reinforced foundation soils. *J Geotech Geoenviron Eng* 130(4):381–390
13. Michalowski RL, You L (1998) Effective width rule in calculations of bearing capacity of shallow footings. *Comput Geotech* 23:237–253
14. Mahiyar H, Patel AN (2000) Analysis of angle shaped footing under eccentric loading. *J Geotech Geoenviron Eng ASCE* 126(12):1151–1156
15. Saran S, Kumar S, Garg K, Kumar A (2007) Analysis of square and rectangular footings subjected to eccentric-inclined load resting on reinforced sand. *J Geotech Geol Eng* 25:123–137. (**Springer Science and Business Med.**)
16. Saran S, Kumar S, Garg K, Kumar A (2008) Model tests on eccentrically and obliquely loaded footings resting on reinforced sand. *Int J Geotech Eng* 2:179–197
17. Sawaf M, Nazir A (2012) Behavior of eccentrically loaded small scale ring footing resting on reinforced layered soil. *J Geotech Geoenviron Eng ASCE* 138(3):376–384
18. Boushehrian J, Hataf N (2003) Experimental and numerical investigation of the bearing capacity of model circular and ring footing on reinforced sand. *Geotext Geomembr* 21:241–256
19. Taiebat H, Carter P (2000) Numerical studies of the bearing capacity of shallow foundations on cohesive soil subjected to combined loading. *Géotechnique* 50(4):409–418
20. Taiebat H, Carter P (2002) Bearing capacity of strip and circular foundations on undrained clay subjected to eccentric loads. *Géotechnique* 52(1):61–64
21. Meyerhof GG (1953) The bearing capacity of foundations under eccentric and inclined loads. *Proceedings of the Conference on Soil Mechanics and Foundation Engineering, Zurich, Switzerland*, pp. 440–453
22. Prakash S, Saran S (1971) Bearing capacity of eccentrically loaded footings. *J Soil Mech Found Eng ASCE* 97(1):95–103
23. Hightner WH, Anders JC (1985) Dimensioning footings subjected to eccentric loads. *J Geotech Eng ASCE* 111(5):659–663
24. Purkayastha RD, Char R (1977) Stability analysis for eccentrically loaded footings. *J Geotech Eng ASCE* 103(6):647–653
25. Janbu N (1957) Earth pressures and bearing capacity calculations by generalized procedure of slices. *Proceedings of the 4th International Conference on Soil Mechanics and Foundation Engineering, London*, pp. 198–207
26. Bowles JE, International Edition (1997) Foundation analysis and design, 5th edn. The McGraw-Hill Companies, Inc, New York
27. Sitharam TG, Sireesh S (2004) Model studies of embedded circular footing on geogrid-reinforced sand beds. *Ground Improv* 8(2):69–75
28. Basudhar PK, Saha S, Deb K (2007) Circular footings resting on geotextile-reinforced sand bed. *Geotext Geomembr* 25:377–384
29. Latha M, Somwanshi A (2009) Effect of reinforcement form on the bearing capacity of square footings on sand. *Geotext Geomembr* 27:409–422
30. Kazi M, Shukla K, Habibi D (2015) Effect of submergence on settlement and bearing capacity of surface strip footing on geotextile-reinforced sand bed. *Int J of Geosynth Ground Eng* 1(4):1–11
31. Maji V, Sowmiyaa V, Robinson R (2016) A simple analysis of reinforced soil using equivalent approach. *Int J Geosynth Ground Eng* 2(16):1–12
32. Biswas A, Ansari M, Kumar Dash S, Krishna A (2015) Behavior of geogrid reinforced foundation systems supported on clay subgrades of different strengths. *Int J of Geosynth Ground Eng* 1(20):1–10
33. Sahoo R (2013) Behaviour of eccentrically loaded shallow foundations on granular soil. Master of Technology thesis, National Institute of Technology, Rourkela.
34. Dhar P, Roy S, Chandra B (2013) Behavior of rigid footing under inclined and eccentric loading. *Ann Pure Appl Math* 5(1):71–81
35. Singh VK, Prasad A, Agrawal RK (2007) Effect of soil confinement on ultimate bearing capacity of square footing under eccentric-inclined load. *EJGE* 12:1–14
36. Shen Z, Feng X, Gourvenec S (2016) Undrained capacity of surface foundations with zero-tension interface under planar V-H-M loading. *Comput Geotech* 73:47–57
37. Foundoukos M, Jardine RJ (2003) Effects of eccentric loading on the bearing capacity of shallow foundations. *BGA International Conference on Foundations, Proceedings of the International Conference Organised by British Geotechnical Association and Held in Dundee, Scotland*, pp. 375–384
38. Richards R, Elms D, Buhdu M (1993) Seismic bearing capacity and settlements of foundations. *J Geotech Eng ASCE* 119(4):662–674
39. Badakhshan E, Noorzad A (2015) Load eccentricity effects on behavior of circular footings reinforced with geogrid sheets. *J Rock Mech Geotech Eng* 7:691–699
40. Helwany S (2007) Applied soil mechanics with ABAQUS applications. Wiley, Hoboken